Available online at www.sciencedirect.com

ScienceDirect

journal homepage: www.elsevier.com/locate/issn/15375110

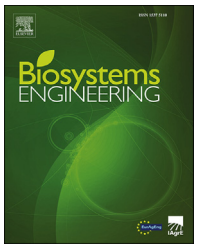

Research Paper

Ammonia emissions from an uncovered dairy slurry storage tank over two years: Interactions with tank operations and meteorological conditions

Thomas Kupper [a,*], *Roy Eugster* [b], *Jörg Sintermann* [b], *Christoph Häni* [a]

[a] *School of Agricultural, Forest and Food Sciences, Bern University of Applied Sciences, Zollikofen, Switzerland*
[b] *Office of Waste, Water, Energy and Air, Canton of Zurich (AWEL), Zurich, Switzerland*

ARTICLE INFO

Article history:
Received 17 July 2020
Received in revised form
23 December 2020
Accepted 8 January 2021
Published online xxx

Keywords:
Manure
Natural crust
Precipitation
Storage
Wind speed

The storage of slurry substantially contributes to the ammonia (NH_3) released from livestock production. This study quantified farm-scale NH_3 emissions from a circular open tank storing dairy cow slurry by means of continuous measurements over two years. Emissions were determined by scaling the product of line-integrated concentration measurements across the tank and wind speed measurements at 10 m height. The resulting data were calibrated to emissions determined using the integrated horizontal flux method. The data analysis was structured according to the main influencing factors: natural crust and meteorological conditions. The average annual emission was 0.065 g NH_3 m^{-2} h^{-1} with a maximum of 1.67 g NH_3 m^{-2} h^{-1}. Annual emissions scaled to total ammoniacal nitrogen (TAN) were 3.3% of the TAN flow into the store. A natural crust on the slurry surface, which was strongly affected by agitation of the tank, diminished the gas release. An increasing time span after agitation led to correspondingly lower emissions. A greater filling level enhanced crust formation and induced an additional drop in emissions. Precipitation reduced emissions by 64%–86% compared to dry weather conditions. Higher wind speed and temperatures increased emissions. The emissions were highest in periods with weak or no crusting of the slurry surface, which covered 40% of the study time, but produced 61% of total emissions. The response of NH_3 emissions to the interactions of influencing factors, which might vary considerably between stores, suggests that these factors require consideration for the determination of emission factors used for inventory reporting.

* *Corresponding author.*
E-mail address: thomas.kupper@bfh.ch (T. Kupper).

https://doi.org/10.1016/j.biosystemseng.2021.01.001

Nomenclature

Au	Autumn
Crust, crusting	See Natural crust
DM	Dry matter
E_{NH3}	NH_3 emission
FL	Filling level
IHF	Integrated horizontal flux
miniDOAS	Differential optical absorption spectroscopy (DOAS) instrument for optical open path measurements of ambient air concentrations of ammonia
Natural crust	A natural crust is formed due to the transport of solids suspended in the slurry being carried to the surface by gas bubbles generated by microbial degradation of the organic material. Evaporation at the surface of the store promotes drying and binding of the particles. These processes induce crust formation (Misselbrook et al., 2005)
PI	Precipitation intensity
S	Season
Sp	Spring
Su	Summer
TAA	Time span after the previous agitation event
TC	Temporal coverage
Temp	Air temperature
u_{10}	Wind speed (m s^{-1}) measured at 10 m height
Wi	Winter
WS	Wind speed

1. Introduction

Livestock production systems producing slurry are widespread in many countries. Slurry stores have been identified as important sources of ammonia (NH_3) emissions (Kupper et al., 2020). Ammonia has a series of negative effects on the quality of air, soil and water, and on ecosystems and biodiversity. Moreover, it indirectly affects the human respiratory tract through the formation of particulate matter (Sutton et al., 2011). In 1999, NH_3 emissions were therefore included in the Gothenburg Protocol to Abate Acidification, Eutrophication and Ground-level Ozone (UNECE, 1999). The parties to this Protocol are obliged to report on their emissions and to control compliance with the national emission ceiling values according to methods provided by EEA (2019) air pollutant emission inventory guidebook. Such methods require the underlying parameters to be based on reliable data. Kupper et al. (2020) showed in their review that wide variability occurs in measurement data, which impedes appropriate determination of emission factors.

Slurry stores are complex systems in which NH_3 emission is driven in many ways (Sommer, Christensen, Schmidt, & Jensen, 2013; Sommer et al., 2006; VanderZaag, Gordon, Glass, & Jamieson, 2008). The principal mechanisms include microbial breakdown of nitrogen (N) in the bulk slurry, which produces dissolved ammonia NH_3(aq) in equilibrium with ammonium NH_4^+(aq). Depending on prevalent chemical equilibria and given that NH_3(aq) and NH_4^+(aq) (denoted as total ammoniacal nitrogen, TAN) are not degraded by microbial processes, these molecules move towards the surface of the store by diffusion and convection. At the slurry–air interface, the molecules pass boundary resistances and disperse into the atmosphere. Transport within the liquid phase depends on the temperature of the slurry (molecular diffusion) and slurry disturbance (advection) induced for example by agitation or by wind shear at the surface. The gas-phase transfer is driven by both temperature and wind speed at the slurry surface (VanderZaag, Amon, Bittman, & Kuczynski, 2015). Surfaces surrounding the emission source that are moist due to rainfall result in sorption of NH_3 as observed by e.g. Petersen, Dorno, Lindholst, Feilberg, and Eriksen (2013). A natural crust on the slurry surface can form, which reduces the transfer of NH_3 between the liquid and the air and provides an environment for microbial activity leading to consumption of NH_3 (Nielsen, Nielsen, Schramm, & Revsbech, 2010). Crust formation depends on the number of fibre particles in the slurry, which is influenced by the slurry type, animal species and their diets, the height of the slurry bulk layer in the stores, meteorological conditions (Smith, Cumby, Lapworth, Misselbrook, & Williams, 2007) and operations at the slurry store.

The complex interactions associated with prevailing meteorological conditions and store operations must be considered when determining emissions (Grant & Boehm, 2015). It is hardly feasible to create conditions at laboratory- or pilot-scale which are equivalent to the real-world (Baldé et al., 2018). Therefore, measurements at farm-scale over an adequate time period are required, since there have been few such investigations.

2. Material and methods

2.1. Farm and storage tank

The investigated slurry tank is situated approximately 70 m west of a dairy farm (Fig. 1). It is a circular open tank of enamelled steel 21 m in diameter and 4.5 m in height with a surface area of 346 m^2, and a capacity of 1558 m^3. The tank is fed from a 100-head dairy house with cubicles, natural ventilation and an adjacent open exercise yard. The dairy housing is located south-east of the storage tank (at approx. 120° N). Wind rarely comes from this direction, i.e. less than 10% of the time. Both the house and the yard have a solid floor, which is regularly cleaned with a scraper. The cubicles are littered with short straw. The slurry was collected in a pit and periodically pumped to the tank via pipes mounted over the rim of the tank. Between 17 May 2016 and 30 January 2017, an immersion pipe was assembled at the outlet of the feed pipe and the slurry entered the tank below the slurry surface. However, due to freezing of the immersion pipe, it was removed at the end of January 2017. A propeller agitator and the extraction pipe were located opposite the feed pipe. There were no other stationary sources, such as farms in the

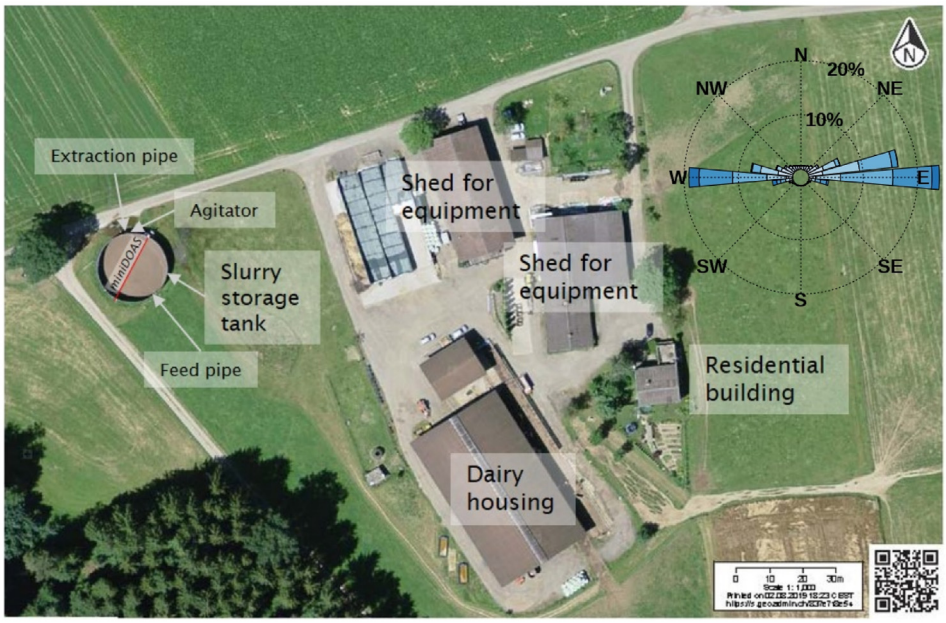

Fig. 1 – Configuration of the slurry tank and the farm (source: https://map.geo.admin.ch) with wind distribution during the measurements. The red line shows the measuring path of the miniDOAS device. (For interpretation of the references to color in this figure legend, the reader is referred to the Web version of this article.)

surrounding area of the tank at less than 700 m distance, which could have affected the measurements. Temporary NH_3 emissions due to agricultural activities (e.g. manure spreading) could have occurred near the tank during the measurements.

2.2. Measurements

2.2.1. NH_3 concentrations and meteorological parameters

A line-integrated measurement of NH_3 concentration was performed at the rim of the tank using a miniDOAS (Sintermann et al., 2016) (Fig. 2). The miniDOAS is an open path device and thus avoids interactions of NH_3 with tubing, inlets, and filters, which provides significant advantages for high measurement accuracy. It operates broadband in the UV range with a time resolution ranging from 20 to 500 ms for individual spectra. In the present study, individual spectra integration times ranged between 200 and 500 ms. These were averaged to 10-min means, from which the corresponding NH_3 concentration was derived by fitting reference spectra to the measurement spectra. The random uncertainty of the concentration measurement is about 1.4% (Sintermann et al., 2016) and for the present experiment on average 3.7 $\mu g\ m^{-3}$ in absolute terms, derived as standard error of the spectral fit. This remained roughly constant over the entire measurement campaign. In addition, in the middle of the tank, a concentration profile 1 m below and 1 m, 2 m and 3 m above the miniDOAS path was measured using passive samplers (Radiello® diffusive samplers (Thimonier et al., 2019)) with an exposure time of one week. At approximately 750 m distance in a north-easterly direction and away from agricultural sources, background concentrations were measured with the same type of passive samplers over periods of four weeks.

The measurements of the wind speed profile were conducted adjacent to the tank (10-min averages) at the same heights as the three passive samplers situated above the miniDOAS path using cup anemometers (Campbell Scientific, Fig. 2). A 3D sonic anemometer (WindMaster™Pro, Gill Instruments Limited, Lymington, UK) was mounted at 10 m height. Two additional cup anemometers were located at the rim of the tank towards the main wind directions of west and north-east by east. A temperature profile was measured (10-min averages) at the rim of the tank and 1 m, 2 m and 3 m above it. The precipitation intensity and the relative air humidity were measured at 10-min intervals at 4.5 m above the bottom of the tank.

The measurements of NH_3 concentrations and meteorological parameters lasted from 30 January 2015 until 18 April 2017 except for the passive sampler data, which covered the time between 5 April 2016 and 18 April 2017. During the measuring period, 88% of the measurement time produced valid data, i.e. simultaneous records from measurements of NH_3 concentration and wind speed.

2.2.2. Operations at the storage tank and sampling of slurry

On 14 August 2015 and 23 March 2017, slurry samples were collected and analysed for dry matter (DM), volatile solids, total nitrogen (N), ammonium-N (NH_4^+-N), phosphorus, potassium, calcium, magnesium and sulfur. From 30 January 2015 until 18 April 2017, operations at the slurry tank (agitation, filling, discharging) were recorded by means of a webcam. In addition, the recorded pictures were used for a visual assessment of the coverage of the tank surface by a natural crust. The filling level of the tank was logged using an optical distant measurement sensor (LIDAR-Lite v3, Garmin, Neuhausen, CH) at 10-min intervals. From August 2016 onwards, the thickness of the natural crust was measured from the rim

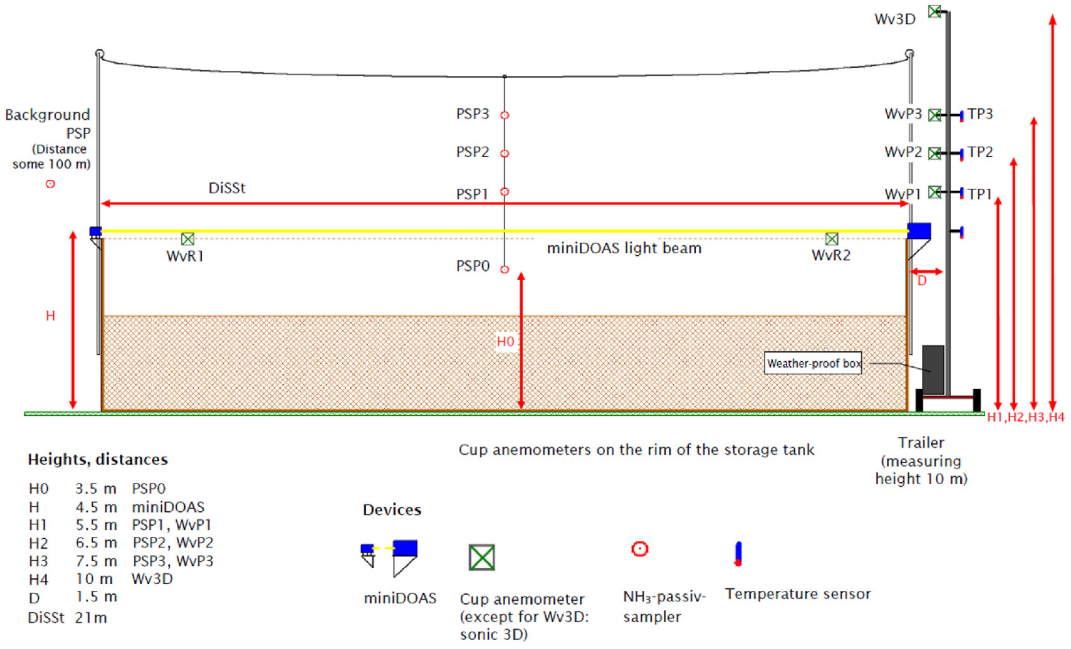

Fig. 2 – Configuration and positions of measurement devices. Concentration measurements of NH_3: miniDOAS, PSP0-PSP3: Radiello® passive samplers. Temperature at the levels of the NH_3 measurements: TP1, TP2, TP3; temperature sensors. Wind speed and turbulence: WvP1, WvP2, WvP3, WvR1-WvR2: cup anemometers; Wv3D: 3D sonic anemometer. H0, H, H1, H2, H3, H4: heights of the devices above the bottom of the tank; DiSSt: length of the miniDOAS path.

of the tank at one position opposite the agitator. The method used is similar to that of Smith et al. (2007). Further information is provided in Supplementary information 1.

2.3. *Emission calculation*

NH_3 emissions (E_{NH3}) were calculated from the linearly scaled product of the 10-min average of the wind speed u_{10}, measured at 10 m height, and the 10-min average of the NH_3 concentration c_{DOAS} provided by the miniDOAS, $E_{NH3} = s_1 + s_2 * u_{10}c_{DOAS}$. This scaling approach assumes that the average horizontal flux $u_{10}c_{DOAS}$ over the path of the miniDOAS scales linearly with the effective emission. The scaling coefficients s_1 and s_2 were derived from parallel measurements of the NH_3 flux using the integrated horizontal flux (IHF) method, e.g. Harper, Denmead, and Flesch (2011) during a period of 371 days. The IHF flux was calculated as weekly averages from profile measurements of the horizontal wind speed at the ridge of the tank and the concentration increase relative to the background at four and five heights in the centre of the tank, respectively. The concentration profile was measured with passive samplers on a weekly basis, whereas the 10-min average values of the wind speed was aggregated to corresponding weekly averages. More information on how the IHF method was employed is provided in Supplementary information 2. The product of u_{10} and c_{DOAS} was calibrated against the measured IHF fluxes (F_{IHF}), whereby both values (u_{10}) and (c_{DOAS}) were averaged over the sampling time of the passive samplers (one week) beforehand (Fig. 3). The scaling coefficients were derived from a robust, linear regression that is symmetric in both F_{IHF} and $u_{10}c_{DOAS}$ (*pbreg* from the R package *deming*; Therneau, 2018).

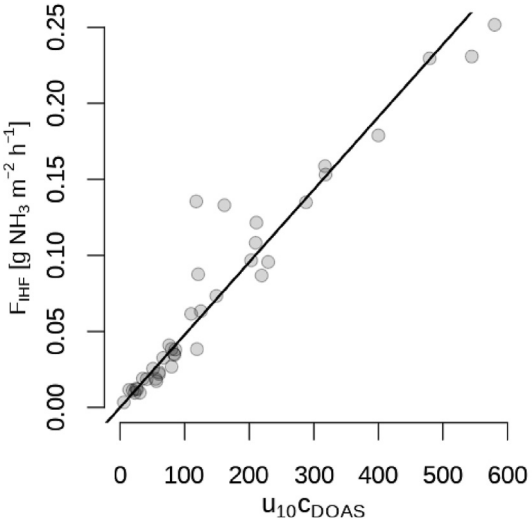

Fig. 3 – Scatterplot with regression line of the robust, linear regression between the IHF emission flux (F_{IHF}) based on weekly average values from the passive samplers and $u_{10}c_{DOAS}$ weekly average values of the product between u_{10} the wind speed (m s^{-1}) at 10 m height and c_{DOAS}, which is the NH_3 concentration in μg m^{-3} measured with the miniDOAS. The regression line corresponds to the final calibration of the NH_3 emission (E_{NH3}) in Eq. (1).

The 10-min estimates of E_{NH3} derived from the miniDOAS measurements are calculated as:

$$E_{NH3} = 1.99*10^{-6} + 4.78*10^{-4}*u_{10}c_{DOAS} \quad (1)$$

where E_{NH3} is given in g NH_3 m^{-2} h^{-1}, u_{10} is given in m s^{-1} and c_{DOAS} in μg m^{-3}.

2.4. Linear regression analysis for influencing factors

We conducted a regression analysis based on the following factors that were hypothesised to substantially influence the level of NH_3 emission from the tank:

i) Time span after agitation: crusting, which acts as a barrier to gas release, occurs at a slurry DM content of ≥40 g L^{-1} (Misselbrook et al., 2005). In the present study, the average DM content was 56 g L^{-1} (Supplementary information 3). In addition to DM, agitation is the most relevant factor for crusting since it destroys the natural crust. Considering that a natural crust builds up with time after an agitation event, we used the time span after slurry agitation as a surrogate for the occurrence of a natural crust. We defined the occurrence of a completely crusted surface as having at least 10 cm of thickness, and thus inducing a relevant reduction of NH_3 emissions (Misselbrook et al., 2005), at least 14 days after agitation. For a time span between one and 14 days after agitation, we assumed a presence of a partly crusted surface or a surface crust of less than 10 cm thickness and a limited decline of NH_3 emissions. Up to one day after agitation was defined as a period without a natural crust where the transport of TAN towards the slurry surface, and thus NH_3 release, is enhanced. In the following text, we use the term "TAA" for the time span after agitation.

ii) Filling level of the tank: with an increasing tank filling level, more fibrous material per m^2 surface is available in the bulk slurry and can move up to the surface, thus enhancing crusting (VanderZaag et al., 2015).

iii) Precipitation intensity, temperature and wind speed: NH_3 emissions are influenced by precipitation (Petersen et al. (2013), temperature and wind speed (Ni, 1999).

For the analysis, ordinary least squares regression was performed. The response variable (NH_3 emission in g m^{-2} h^{-1}) was the (10-min) emission estimates from the mini-DOAS measurements (E_{NH3}), transformed by a log 10 transformation. The independent variables were the TAA provided as categories ≤1 d, 1–14 d and ≥14 d after agitation, the filling level of the tank (two categories: ≤1 m and >1 m), precipitation intensity (three categories: 0 mm h^{-1}, 0.1-<2 mm h^{-1} and 2–10 mm h^{-1}), air temperature at the upper rim of the tank $T_{4.5m}$ (in °C) and the log10 of wind speed at 10 m height U_{10m} (in m s^{-1}). Interaction between the TAA categories and the other predictor variables (filling level, precipitation intensity, air temperature and wind speed) was included to reflect different effect sizes of these variables for different TAA categories. The defined categories for TAA, filling level and precipitation intensity were determined based on expert judgment.

The regression equation is given by

$$\log_{10}(E_{NH3}) = \alpha_{base} + A_{TAA} + A_{FL} + A_{PI} + B_{T_{4.5m}} * T_{4.5m} + B_{U_{10m}} * \log_{10}(U_{10m}) \quad (2)$$

where

$$A_{TAA} = \begin{cases} 0\ ,\ if\ TAA=' \le 1\ d' \\ \alpha_{1-14\ d}\ ,\ if\ TAA='1-14\ d' \\ \alpha_{\ge 14\ d}\ ,\ if\ TAA=' \ge 14\ d' \end{cases}$$

$$A_{FL} = \begin{cases} 0\ ,\ if\ FL=' \le 1\ m' \\ \alpha_{FL>1\ m,\le 1\ d}\ ,\ if\ FL=' > 1\ m'\ and\ TAA=' \le 1\ d' \\ \alpha_{FL>1\ m,1-14\ d}\ ,\ if\ FL=' > 1\ m'\ and\ TAA='1-14\ d' \\ \alpha_{FL>1\ m,\ge 14\ d}\ ,\ if\ FL=' > 1\ m'\ and\ TAA=' \ge 14\ d' \end{cases}$$

$$A_{PI} = \begin{cases} 0\ ,\ if\ PI='0\ mm\ h^{-1}' \\ \alpha_{PI_{med},\le 1\ d}\ ,\ if\ PI='0.1-<2\ mm\ h^{-1}'\ and\ TAA=' \le 1\ d' \\ \alpha_{PI_{med},1-14\ d}\ ,\ if\ PI='0.1-<2\ mm\ h^{-1}'\ and\ TAA='1-14\ d' \\ \alpha_{PI_{med},\ge 14\ d}\ ,\ if\ PI='0.1-<2\ mm\ h^{-1}'\ and\ TAA=' \ge 14\ d' \\ \alpha_{PI_{hi},\le 1\ d}\ ,\ if\ PI='2-10\ mm\ h^{-1}'\ and\ TAA=' \le 1\ d' \\ \alpha_{PI_{hi},1-14\ d}\ ,\ if\ PI='2-10\ mm\ h^{-1}'\ and\ TAA='1-14\ d' \\ \alpha_{PI_{hi},\ge 14\ d}\ ,\ if\ PI='2-10\ mm\ h^{-1}'\ and\ TAA=' \ge 14\ d' \end{cases}$$

$$B_{T_{4.5m}} = \begin{cases} \beta_{T_{4.5m},\le 1\ d}\ ,\ if\ TAA=' \le 1\ d' \\ \beta_{T_{4.5m},1-14\ d}\ ,\ if\ TAA='1-14\ d' \\ \beta_{T_{4.5m},\ge 14\ d}\ ,\ if\ TAA=' \ge 14\ d' \end{cases}$$

and

$$B_{U_{10m}} = \begin{cases} \beta_{U_{10m},\le 1\ d}\ ,\ if\ TAA=' \le 1\ d' \\ \beta_{U_{10m},1-14\ d}\ ,\ if\ TAA='1-14\ d' \\ \beta_{U_{10m},\ge 14\ d}\ ,\ if\ TAA=' \ge 14\ d' \end{cases}$$

are the corresponding coefficients.

The log–linear relationship between the emission and the influencing parameters implies that the effect of a parameter is larger for higher emission values, i.e. relative to the emission value.

3. Results and discussion

3.1. Operations at the storage tank

To evaluate the TAA as a surrogate for crusting, we measured the crust thickness at different time spans after agitation (Supplementary information 1). Thirteen measurements revealed a crust with ≥10 cm thickness after ≥14 days after the last previous agitation, which corresponds to 42% of the total of 31 measurements. In ten cases (32% of measurements), no crust or a crust with less than 10 cm thickness occurred at less than 14 days after the last previous agitation. But, in four cases (13% of measurements), a crust with ≥10 cm thickness was present after less than 14 days, i.e. after 10 days on average. In four cases again, a natural crust of less than 10 cm of thickness existed after more than 14 days. This was in late autumn 2016 when the filling level was below 0.5 m and thus little fibrous material was available to form a stable crust (Supplementary information 1, Fig. 1). Overall, 74% of the measurements were able to correctly allocate the state of crusting to the definition of TAA 1–14 d (weak or partial crusting) and ≥14 d

(completely crusted surface). Additionally, periodic on-site inspections and the visual assessment of the webcam pictures confirmed that two weeks after agitation, the whole tank surface was covered by a natural crust. Wood, Gordon, Wagner-Riddle, Dunfield, and Madani (2012) showed in a pilot-scale study that the emission-reducing effect can be partly offset if cracks occur in the crust. It was not possible to include crack occurrence in the crust and to assess its impact on emissions.

VanderZaag et al. (2015) suggested that crusting is enhanced by an increasing tank filling level. Specific numbers regarding this influencing factor are not available. In our study, the filling level was on average 1.4 m ranging from 0.2 m to 4.1 m with higher levels in winter and spring (Fig. 4).

Both agitation and filling of the tank destroy the natural crust. Over the entire measuring period, one or two agitation events occurred per month on average (Table 1; Supplementary information 1, Table 1). The operation time of the agitator was 178 h in total and on average ca. 3.5 h per event. The operation duration per year reached ca. 70 h. Filling of the tank occurred approximately twice per month. The average duration of one filling event was ca. 2.5 h. Emptying of slurry might also impair the crust but mostly coincides with agitation and is thus not separately addressed here.

Data on tank operations from the literature is scarce. Approximately 20 agitation events occur per year at ca. 30% of Swiss farms, while the remaining 70% agitate the slurry tank once per month or less (Kupper, Bonjour, & Menzi, 2015). Kariyapperuma et al. (2018) reported two agitation events and two periods with slurry addition over one year. The same was found for a farm in Canada, where Baldé et al. (2018) reported agitation only before removal of slurry, which occurred in autumn. This suggests that slurry agitation and tank filling occurred much more frequently at the investigated farm than has been found in other production systems.

3.2. *Emissions from the storage tank*

Figure 4 shows the NH_3 emissions over the two-year measuring period, the operations at the tank and the course of meteorological parameters. The yearly average emission, based on mean values from winter, spring, summer and autumn included in the entire measurement period (30 January 2015 to 18 April 2017), was 0.065 g NH_3 m^{-2} h^{-1} ± 0.110 g NH_3 m^{-2} h^{-1} with a range between a minimum of

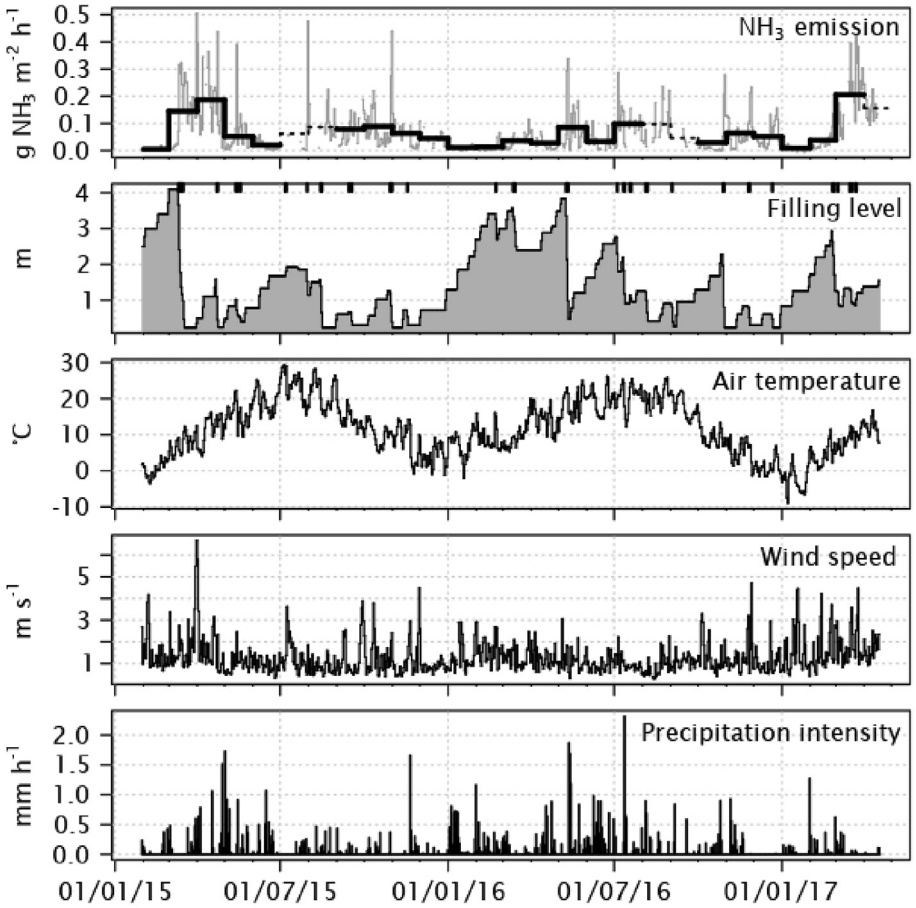

Fig. 4 – NH_3 emissions (g NH_3 m^{-2} h^{-1}) from the storage tank between 30 January 2015 and 18 April 2017: the daily (grey line) and monthly (bold black line) average values are provided. Monthly averages based on less than 75% of the time of the months are presented by a dotted line. Below, the daily averages of the influencing factors are shown: filling level of the tank (m), with lines at the top of the graph indicating the agitation events, air temperature (°C), wind speed (m s^{-1}) and precipitation intensity (mm h^{-1}).

Table 1 – NH_3 Emissions from the storage tank. The measuring periods are aggregated to the seasons (S) winter (Wi), spring (Sp), summer (Su) and autumn (Au) and the average over all seasons (All). Three winter and spring seasons and two summer and autumn seasons are included. The temporal coverage (TC) is given as the number of hours and the percentage coverage of the measuring period duration. The emissions are given in g NH_3 m^{-2} h^{-1} as average, standard deviation (SD) and range between the minimum and maximum of 10-min measuring intervals. Parameters related to 10-min measuring intervals: average air temperature (Temp) in °C measured at 4.5 m height; wind speed (WS) in m s^{-1} measured at 10 m height; precipitation: proportion of measurement intervals with precipitation measured at 1.0 m height in %; precipitation sum (∑) in mm, measured at 4.5 m height; average frequency of agitation and filling of the tank and average duration per event in h, average filling level (FL) of the tank in m and time span after agitation: percentage distribution of ≤1 day, 1–14 days and ≥14 days and average number of days after the last previous agitation event. The TAN flow into storage tank is given in kg TAN.

S[a]	TC[b]	NH_3-emission			Temp[c]	WS[d]	Precipitation[e]		Agitation	Filling	FL[f]	Time span after agitation				TAN-flow into tank
	Number h/%	Average	SD	Range	Average				Average number of events/duration in h		m	≤1 d	1–14 d	≥14 d	Days	
		g NH_3 m^{-2} h^{-1}			°C	m s^{-1}	%	∑ (mm)				%	%	%		kg TAN
Wi	4673 h/72%	0.025	0.043	<0.001–0.958	3.5	1.4	13	124	1.3/6.5 h	6.7/3.0 h	1.8	2	16	82	38.9	1320
Sp	5096 h/77%	0.110	0.154	<0.001–1.403	12.3	1.5	15	231	7.0/3.5 h	6.3/2.5 h	1.6	10	46	44	15.6	1193
Su	3319 h/75%	0.064	0.104	<0.001–1.669	20.3	1.0	11	219	4.5/3.1 h	7.0/1.6 h	1.4	6	38	56	19.2	1241
Au	3934 h/90%	0.063	0.085	<0.001–0.800	10.3	1.3	11	157	5.0/2.6 h	6.0/3.2 h	0.8	5	37	58	19.6	1218
All	17,022 h/78%	0.065	0.110	<0.001–1.669	11.6	1.3	12	730	17.8/3.4 h	26/2.6 h	1.4	6	34	60	23.3	4972

[a] S: season: Wi: winter, Sp: spring, Su: summer, Au: autumn.
[b] TC: temporal coverage in h; %: percentage temporal coverage of the measuring period duration.
[c] Temp: air temperature.
[d] WS: wind speed.
[e] Precipitation %: proportion of measurement intervals with precipitation; precipitation ∑: precipitation sum in mm; the percentage denote the proportion of precipitation captured during 10-min measuring intervals with valid emission data relative to the total precipitation sum.
[f] FL: filling level.

<0.01 g NH_3 m^{-2} h^{-1} and a maximum of 1.67 g NH_3 m^{-2} h^{-1} (Table 1). For 2015 and 2016, the average emissions were 0.077 NH_3 m^{-2} h^{-1} ± 0.128 NH_3 m^{-2} h^{-1} and 0.048 NH_3 m^{-2} h^{-1} ± 0.077 g NH_3 m^{-2} h^{-1}, respectively (Supplementary information 5). Due to the simplified emission calculation by the scaling approach described in section 2.3, the uncertainty in emission values could be higher than the variation indicated by the standard deviation.

The emission trends within a day and during the four seasons correspond to the expected pattern, with highest emissions between sunrise and sunset, particularly in the early afternoon, and in warm seasons (Fig. 5), as previously observed in other studies (Baldé et al., 2018; Grant, Boehm, Lawrence, & Heber, 2013). The diurnal emission patterns were most pronounced for warmer seasons, while diurnal emission variability was small during wintertime.

The emission values are in line with the range reported in the literature. A recent literature review by Kupper et al. (2020) determined baseline emissions for untreated cattle slurry stored uncovered in tanks of 0.08 g NH_3 m^{-2} h^{-1} (range between lower and upper 95% confidence interval: 0.07–0.09 g NH_3 m^{-2} h^{-1}). These values are based on emission measurements at pilot-scale and farm-scale. For the subset of data from farm-scale studies, the review determined emissions of 0.09 g NH_3 m^{-2} h^{-1} (range between lower and upper 95% confidence interval: 0.05–0.13 g NH_3 m^{-2} h^{-1}).

Annual emissions per unit of TAN or more precisely, scaled to the TAN flow into the store, is commonly used for inventory calculations (EEA, 2019). For this, the annual flow of TAN into the store and the annual NH_3 loss therefrom are required. We calculated the TAN flow by using the slurry production of 3583 m^3 y^{-1}, which is based on the sum of the measured changes in the filling level and the tank surface. The volume of produced slurry compares well with the average production of 3680 m^3 y^{-1} derived from Richner et al. (2017), given a 1:0.6 dilution of the slurry with water, the slurry dry matter content of 56 g L^{-1} of the present study and a standard dry matter value of 90 g L^{-1} for undiluted cattle slurry, according to Richner et al. (2017). Combined with the TAN content of the slurry of 1.39 g L^{-1} (Supplementary information 3), a flow of 4972 kg TAN y^{-1} into storage was calculated. Based on the average emission of 0.065 g NH_3 m^{-2} h^{-1} and the tank surface area of 346 m^2, the cumulative annual NH_3 loss from the tank is 163 kg NH_3–N y^{-1}, which corresponds to an annual emission of 3.3% scaled to the TAN flow into the store. This is substantially lower than the value from EEA (2019), which provides an emission factor of 25% of TAN as Tier 2 default value for cattle slurry. Kupper et al. (2020) reported in their review emissions of 16% of TAN based on almost exclusively pilot-scale studies.

For the calculation of emissions from storage per unit of TAN, the residence time of slurry in the store is crucial for pilot-scale studies which start with the filling of an experimental tank with slurry and end with the termination of the emission measurements. The initial amount of slurry with a given TAN content in the experimental tank constitutes the initial amount of TAN. The relative TAN loss increases proportional to the residence time since the measured emission rates are accounted for over a longer time period on an amount of TAN present in the store. The residence time

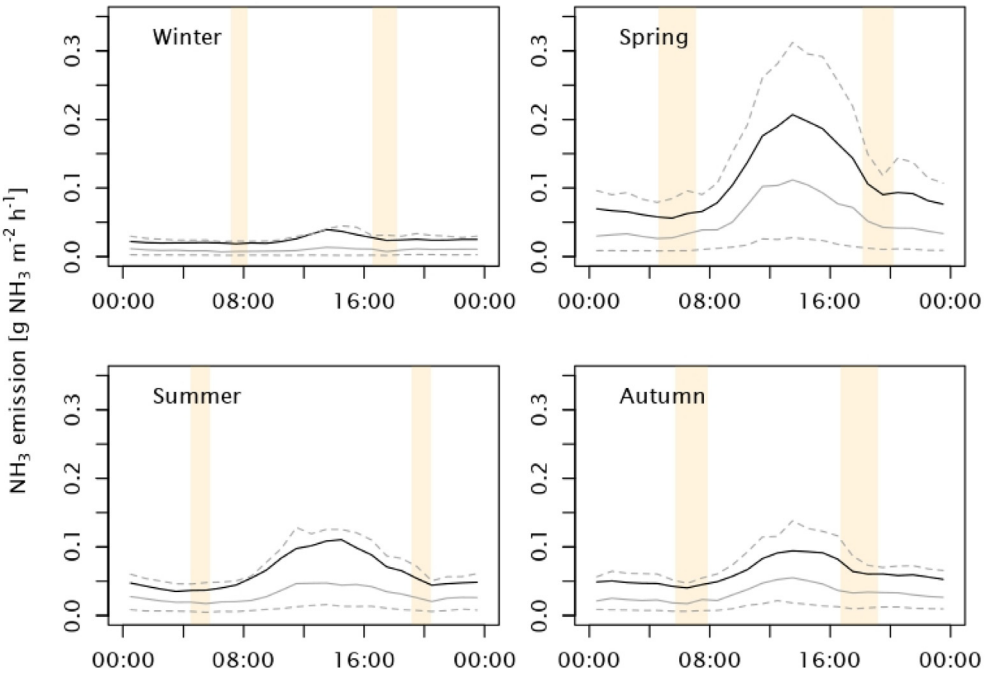

Fig. 5 – Diurnal pattern of NH_3 emissions (g NH_3 m^{-2} h^{-1}) from the storage tank over the seasons captured between 30 January 2015 and 18 April 2017. The 25% percentile (lower dashed grey line), the median (grey solid line), the average (black line) and the 75% percentile (upper dashed grey line) are shown. The time of day is UTC+1. The timespan of sunrise and sunset is highlighted in orange (Agafonkin & Thieurmel, 2018). (For interpretation of the references to color in this figure legend, the reader is referred to the Web version of this article.)

assumed by Kupper et al. (2020) is equivalent to the duration of the experiments, which was on average approximately 150 days. For our study, a tank surface area of 346 m^2 and an average slurry volume in the tank of 485 m^3 occur given the 1.4 m average filling level (Table 1). Our calculation yields a residence time of slurry in the tank of 51 days. This and the higher emissions of pilot-scale studies (approximately 0.10 g NH_3 m^{-2} h^{-1}) explain the difference in emissions from storage per unit of TAN between this study and the review by Kupper et al. (2020).

The emission factor provided by EEA (2019) is based on annual average emissions on an area basis related to a store with a 3 m filling level and an average TAN concentration of the slurry obtained from underlying studies. This approach does not imply a turnover of slurry across the store. The procedure given by EEA (2019), which was employed for the slurry store of the present study (i.e. emission: 0.065 g NH_3 m^{-2} h^{-1}; filling level: 1.4 m; TAN content of slurry: 1390 g m^{-3}) would produce an emission of 29% of TAN (calculation provided in Supplementary information 4). This is similar to the EEA (2019) emission factor which is 25% of TAN. Here, the difference between the EEA (2019) approach and this study is mainly due to the lower emissions on an area basis and slurry filling level of this study compared to the corresponding underlying data of EEA (2019) provided by Sommer, Webb, and Hutchings (2019). The low filling level and the short residence time of slurry found in the present study are due to frequent emptying of the tank. This can be considered as typical for production systems where slurry is commonly applied to grassland after fodder harvest, and such systems are likely to be used in conditions with favourable herbage production and thus high cutting frequency.

At farm-scale, a store is never completely empty or is evacuated only a few times during the year. For farm-scale studies, the TAN load in the store is based on the slurry volume entering the store which can be determined from the sum of changes in filling level over the year and the TAN content of the slurry. The store surface area and the annual average emission on an area basis yield the total NH_3 loss. In a study conducted at farm-scale, Baldé et al. (2018) calculated a loss of 16% of TAN for untreated cattle slurry stored uncovered with storage emptying in spring and autumn. They reported a higher emission level (0.11 g NH_3 m^{-2} h^{-1}) but a comparable chemical composition of the slurry to that found in the present study. Under the assumption that the emission on an area basis is independent of the TAN load in the store and the store surface area, we can extrapolate the emission of Baldé et al. (2018) (0.11 g NH_3 m^{-2} h^{-1}) to our store with the flow into store of 4972 kg TAN y^{-1} and the surface area of 346 m^2. This results in an emission of 5.5% of TAN. The remaining difference between the 5.5% and the 3.3% of TAN of our study is due to the emission on an area basis which is higher by a factor of 1.7 in Baldé et al. (2018). These authors stated that the employed micrometeorological techniques are biased towards windier conditions due to the removal of measurement data at low wind-speeds which would likely result in an overestimation of the true annual NH_3 emission. The store which they investigated was an earthen basin with an area size of 6665 m^2. The turbulence at the slurry surface and thus the emissions are likely to be substantially higher under these conditions than at our store, where the slurry surface was on average 3.1 m below the upper rim of the tank walls. Consequently, the reported 16% of TAN loss is substantially higher than that of the present study. Apart from the emission level, differences in TAN loads and surface area could explain the discrepancies in emissions per unit of TAN between the two studies.

These considerations illustrate that a large range in emissions from slurry storage per unit of TAN occurs in the literature, in the EEA (2019) air pollutant emission inventory guidebook and in farm-scale studies. In principle, emissions per unit of TAN depend on the annual TAN flow into the store, the store surface area and the annual average emission on an area basis, assuming that these three parameters are mostly independent of each other. The annual TAN flow into the store is also related to the slurry residence time in the store or the slurry turnover rate per year. The latter is given by the TAN flow into the store due to the frequency of slurry filling and emptying. These parameters vary largely among the different approaches and also fluctuate between farm production systems and store types. This variability should be further explored and included in the approaches for emission calculation to achieve adequate emission factors based on the TAN flow for inventory calculations.

3.3. *Influence of operations and meteorological conditions on emissions from storage tank*

3.3.1. *Overview*

We analysed the impact of crusting, which is affected by operations at the tank, and meteorological conditions on emissions based on the classification given in Fig. 6. Emissions in dry weather conditions are progressively reduced with TAA 1–14 d and ≥14 d compared to TAA ≤1 d at identical categories for filling level, wind speed and temperature (Fig. 6A). This is related to the enhanced formation of a natural crust. When precipitation occurs, sorption of NH_3 onto wet areas and dilution of the TAN concentration at the emitting surface seem to dominate over the emission-reducing effect of crusting. This is reflected by unstructured emission levels independent of the TAA when precipitation occurs (Fig. 6B and C). For TAA ≥14 d, emissions at a filling level ≤1 m exceed those associated with a filling level >1 m for all comparisons. This suggests that lower emissions at a higher tank filling level are related to the occurrence of a natural crust. A similar systematic emission pattern does not occur for filling levels ≤1 m and >1 m for TAA ≤1 d and 1–14 d, respectively. Here, crusting had probably not yet occurred or was incomplete.

In the present study, a TAA ≥14 d, representing the occurrence of a natural crust, prevailed for over 60% of the experimental period. During this time, the average emission reached 0.044 g NH_3 m^{-2} h^{-1}, which resulted in 39% of the total emissions. Although the tank exhibited a non-crusted or partly crusted surface for only 40% of the time, these conditions were associated with 61% of the total emissions, with an average emission level of 0.103 g NH_3 m^{-2} h^{-1}. This illustrates the effect of a surface crust on the emission level from slurry storage.

The emissions are higher at wind speed >1 m s^{-1} than at wind speed ≤1 m s^{-1} for almost all comparisons, as shown in

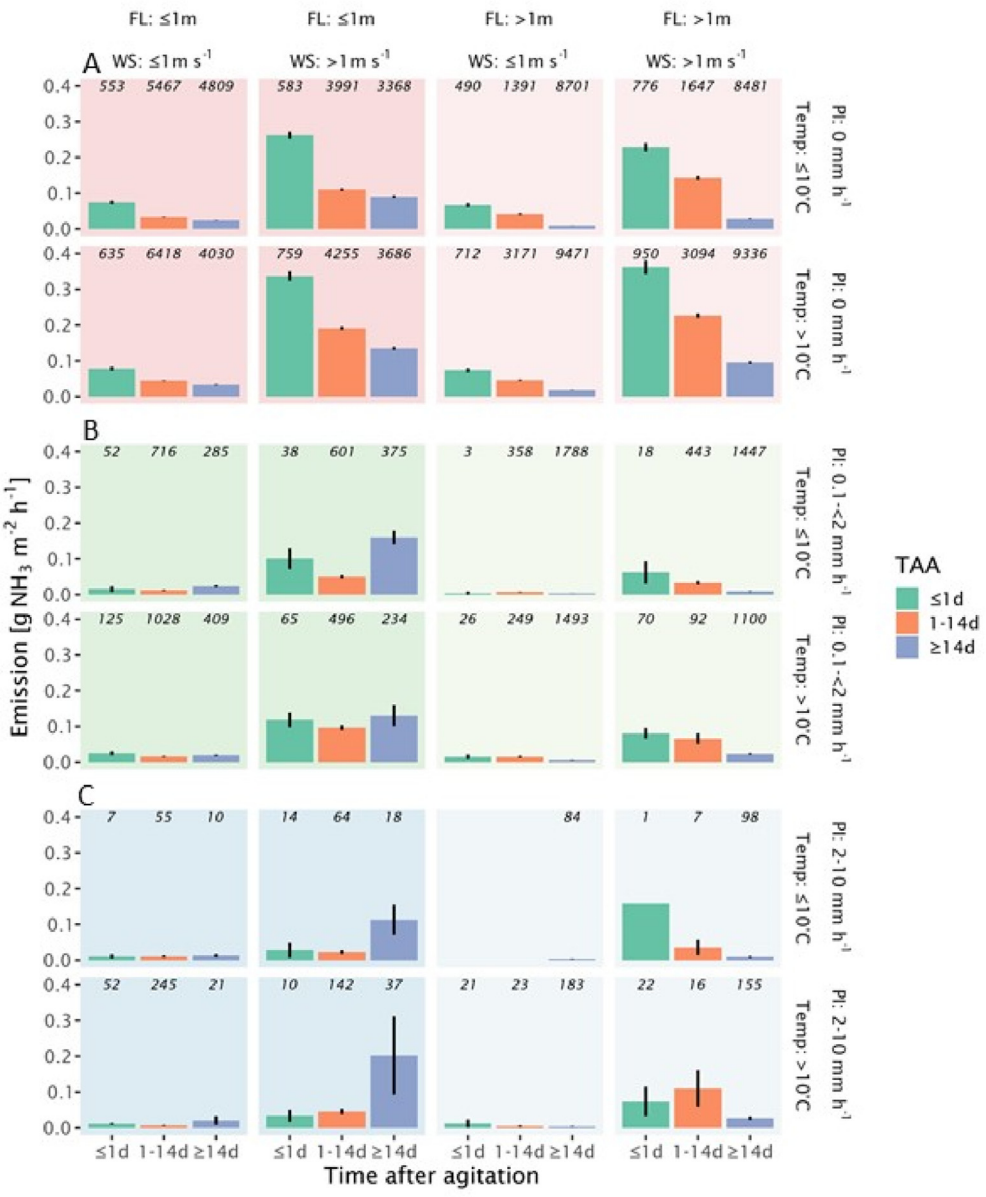

Fig. 6 – Average ammonia emissions in g NH_3 m^{-2} h^{-1} for the given combinations of influencing factors based on measurements between 30 January 2015 and 18 April 2017. The vertical bars show the standard error determined by bootstrapping (Efron, 1987). The plots are outlined according to the influencing factors: the three bars indicate the time span after the previous agitation event ≤1 d, 1–14 d and ≥14 d (TAA), which are surrogates for no natural crust present, weak or partial crusting and well-developed natural crust, respectively. The horizontal classification includes the filling level, FL (≤1 m; >1 m), and the wind speed, WS (≤1 m s^{-1}; >1 m s^{-1}). The vertical classification comprises precipitation intensity, PI: A: 0 mm h^{-1}; B: 0.1-<2 mm h^{-1}; C: 2–10 mm h^{-1}) and the air temperature, Temp (≤10 °C, >10 °C). The numbers at the top of the subplots indicate the number of 10-min measuring intervals.

Fig. 6. Similarly, at temperatures >10 °C, emissions are mostly higher than at ≤10 °C, although this is less pronounced when precipitation occurs. Both effects are due to physical-chemical mechanisms described by Ni (1999) and Sommer et al. (2006).

Meteorological conditions and crusting of the tank surface can also explain the occurrence of the highest emissions in spring 2015 and 2017 with 0.126 NH_3 m^{-2} h^{-1} ± 0.176 NH_3 m^{-2} h^{-1} and 0.187 NH_3 m^{-2} h^{-1} ± 0.163 g NH_3 m^{-2} h^{-1} (Supplementary information 5). This contrasts with the analysis of Kupper et al. (2020), who reported an emission increase in the order of cold < temperate < warm season. In the present study, the greater average wind speed (spring: 1.5 m s^{-1}; summer: 1.0 m s^{-1}) and the lower average TAA for spring (spring: 15.6 days; summer: 19.2 days; Table 1) were factors enhancing emissions in spring but less so in summer. A TAA ≥14 d, which occurs in both spring and summer, suggests a well-developed crust that mitigates emissions. Figure 7 shows that the mitigation effect of the crust further increased beyond 14 days after agitation, which predominately applies to summer when emissions are lower than in spring. The

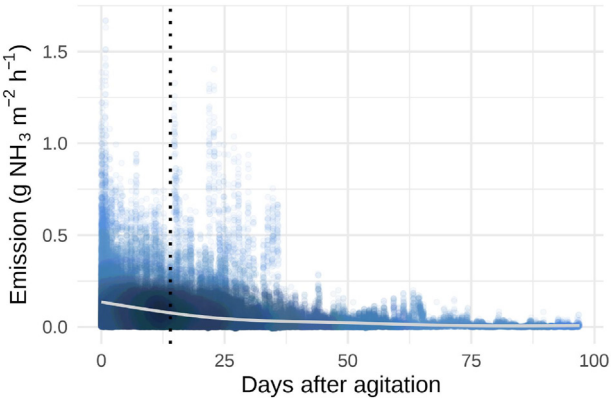

Fig. 7 – NH_3 emissions (g NH_3 m^{-2} h^{-1}) from the storage tank after agitation in days. The blue dots show the individual emission values and the solid line indicates the locally smoothed trend. The vertical dotted line shows 14 days after agitation. (For interpretation of the references to color in this figure legend, the reader is referred to the Web version of this article.)

temperature was higher in summer, which would have led to greater emissions. But Fig. 6 and the linear regression analysis show that the effect of wind speed was stronger than that of temperature.

3.3.2. *Linear regression analysis*

The analysis in the previous paragraph illustrates the emission response to both operations at the tank and meteorological conditions. In addition, the employed regression model provides a quantitative analysis of the observed effects, including interactions between them. The selected independent variables are key parameters derived from the physical-chemical mechanisms driving emissions (Misselbrook et al., 2005; Ni, 1999).

The results of the regression analysis are summarised in Table 2, which shows the coefficients associated to a covariate with the corresponding standard error. The base case is defined as follows: TAA: ≤1 d, filling level (FL): ≤1 m, precipitation intensity (PI): 0 mm h^{-1}, air temperature at 4.5 m: 0 °C, wind speed u10 (at 10 m height): 1 m s^{-1}. The NH_3 emission for the base case is then according to Eq. (2). and Table 2:

$$E_{NH3} = \log_{10}\alpha_{base}\ i.e.\ 10^{-0.99} = 0.1\ g\ NH_3\ m^{-2}\ h^{-1}$$

The "Relative effects" column shows the percentage by which an emission changes relative to the base within the three TAA categories for the filling level >1 m, the two classes of precipitation intensity 0.1-<2 mm h^{-1} and 2–10 mm h^{-1}, air temperature per increase by 1 °C and when doubling the wind speed. All investigated effects are statistically significant ($p < 0.05$; Table 2).

To illustrate the regression analysis, emission estimates for some conditions are provided: example "a" TAA = '≤1 d', FL = '>1 m', PI = '0 mm h^{-1}', air temperature = 15 °C and wind speed = 1 m s^{-1} is calculated as $10^{-0.99\ -\ 0.12+15*0.008}$, which is equal to 0.102 g NH_3 m^{-2} h^{-1}. Given the conditions of example "a", but after 14 days after agitation (TAA = '≥14 d'), the emission is calculated as $10^{-0.99\ -\ 0.61\ -\ 0.58+15*0.025}$, which is equal to 0.016 g NH_3 m^{-2} h^{-1}, corresponding to −85% (Table 2: combining the relative effects of TAA = '≥14 d' (−75%), FL = '>1 m' given TAA = '≥14 d' (−74%) and air temperature equal to 15 °C when TAA = '≥14 d' and not TAA = '≤1 d' (15 * (6%−1.9%) = +61.5%)). Another example, given again conditions for "a" but with a wind speed = 2 m s^{-1} (+100% compared to conditions "a"), the emission increases by +100% (Table 2 relative effect of wind speed given TAA = '≤1 d') to 0.205 g NH_3 m^{-2} h^{-1} ($10^{-0.99\ -\ 0.12+15*0.008+\log10(2)*1.00}$).

The effect related to time after agitation clearly emerges. Emissions for the TAA 1–14 d were lower by 65% and ≥14 d by 75% than those for TAA ≤1 d (Table 2), which supports the approach of TAA as a surrogate for crusting and the related emission decrease. VanderZaag et al. (2015) state that a natural crust can lead to an emission reduction of 40%. Misselbrook et al. (2005) found emissions lower by 50% due to crusting in an experiment conducted at pilot scale. Grant and Boehm (2015) reported a reduction in emissions from two lagoons at a farm by 49% and 5%, respectively. These numbers suggest that the influence of crusting might vary substantially, probably due to differing coverage of the slurry surface by and a varying structure (such as thickness or presence of cracks) of the crust (Wood et al., 2012).

A filling level >1 m induced an emission reduction which was highest for TAA≥14 d (74% reduction). An increasing filling level decreases the surface area to volume ratio. Slurry stores with a low surface area to volume ratio are recommended for NH_3 emission mitigation as they minimise the emitting surface and enlarge the distance that NH_3(aq)/NH_4^+(aq) must diffuse before reaching the slurry surface. With a filling level >1 m, more fibrous material is available to form a crust (Smith et al., 2007; VanderZaag et al., 2015). The lower emission level at a higher filling level is thus in agreement with the literature.

Precipitation reduced emissions by 64%–86% with a greater decrease at a higher intensity (2–10 mm h^{-1}). The reduction was lower for TAA ≥14 d. These outcomes are in line with the results of Petersen et al. (2013), who found lower NH_3 emissions from pig slurry exposed to ambient weather conditions than from the treatment where rainfall had been excluded. Although rain exerts a strong influence on the emission level, its effect is assumed to be rather episodic and, therefore, the influence on total yearly emissions will be limited due to the low proportion of time over the year with precipitation – in this study, only 12% of the measuring intervals exhibited occurrence of precipitation (Table 1, Supplementary information 5).

The emissions became greater with increasing air temperatures. This is due to the enhanced transport of dissolved ammonia in the bulk slurry towards the emitting surface with higher temperatures (Ni, 1999; Sommer et al., 2013). The relative effect was lowest directly after agitation, i.e. TAA ≤1 d, with 1.9% rise in emission per air temperature increase by 1 °C. At TAA 1–14 d and ≥14 d, the effect sizes were 4.7% and 6.0% emission rise per increase of air temperature by 1 °C, respectively.

Increasing wind speed leads to enhanced advective transport at the emitting surface and thus promotes emissions (Ni, 1999). Moreover, it can increase the transport of TAN from the bulk slurry to the store's surface because of the effect of wind

Table 2 – Effect size of regression coefficients (Coeff.), standard error of the effect size (SE (Coeff)), % change in emission per unit change in covariate (Relative effect), relative to the reference based on the linear regression analysis. The coefficients are allocated according to Eq. (2). t, p: test statistics and p-value of the two-sided t-tests. Sig.: significant results of the t-tests (significance level $\alpha = 0.05$) are labelled with an asterisk *.

TAA	Covariates	Variable	Coeff	SE (Coeff)	Relative effect	t	p	Sig.
Base[a]	Base a	α_{base}	−0.99	0.01	–	−71.53	0.000	*
1–14 d	–	$\alpha_{1-14\ d}$	−0.45	0.01	−65%	−30.54	0.000	*
≥14 d	–	$\alpha_{\geq 14\ d}$	−0.61	0.01	−75%	−41.65	0.000	*
≤1 d	FL > 1 m	$\alpha_{FL>1\ m,\leq 1\ d}$	−0.12	0.01	−23%	−9.19	0.000	*
1–14 d	FL > 1 m	$\alpha_{FL>1\ m,1-14\ d}$	−0.06	0.02	−12%	−3.08	0.002	*
≥14 d	FL > 1 m	$\alpha_{FL>1\ m,\geq 14\ d}$	−0.58	0.02	−74%	−31.78	0.000	*
≤1 d	PI 0.1-<2 mm h^{-1}	$\alpha_{PI_{med},\leq 1\ d}$	−0.66	0.03	−78%	−26.41	0.000	*
1–14 d	PI 0.1-<2 mm h^{-1}	$\alpha_{PI_{med},1-14\ d}$	−0.57	0.04	−73%	−15.62	0.000	*
≥14 d	PI 0.1-<2 mm h^{-1}	$\alpha_{PI_{med},\geq 14\ d}$	−0.44	0.04	−64%	−12.38	0.000	*
≤1 d	PI = 2–10 mm h^{-1}	$\alpha_{PI_{hi},\leq 1\ d}$	−0.85	0.04	−86%	−19.74	0.000	*
1–14 d	PI = 2–10 mm h^{-1}	$\alpha_{PI_{hi},1-14\ d}$	−0.81	0.06	−85%	−12.64	0.000	*
≥14 d	PI = 2–10 mm h^{-1}	$\alpha_{PI_{hi},\geq 14\ d}$	−0.44	0.06	−64%	−6.86	0.000	*
≤1 d	Air temperature	$\beta_{T_{4.5m},\leq 1\ d}$	0.008	0.001	+1.9%[b]	9.46	0.000	*
1–14 d	Air temperature	$\beta_{T_{4.5m},1-14\ d}$	0.020	0.001	+4.7%[b]	15.82	0.000	*
≥14 d	Air temperature	$\beta_{T_{4.5m},\geq 14\ d}$	0.025	0.001	+6.0%[b]	20.77	0.000	*
≤1 d	$\log_{10}$(Wind speed)	$\beta_{U_{10m},\leq 1\ d}$	1.00	0.01	+100%[c]	69.15	0.000	*
1–14 d	$\log_{10}$(Wind speed)	$\beta_{U_{10m},1-14\ d}$	0.97	0.02	+96%[c]	45.71	0.000	*
≥14 d	$\log_{10}$(Wind speed)	$\beta_{U_{10m},\geq 14\ d}$	0.92	0.01	+89%[c]	43.96	0.000	*

[a] The Base covariates are defined as time after agitation (TAA): ≤1 d, filling level (FL): ≤1 m, precipitation intensity (PI): 0 mm h^{-1}, air temperature at 4.5 m: 0 °C, wind speed at 10 m height: 1 m s^{-1}.
[b] Change per air temperature increase of 1 °C.
[c] The relative effect of covariate wind speed is proportional to the relative change in wind speed. The values provided represent a relative increase in wind speed of +100% (i.e. doubling of wind speed).

shear and subsequent mixing of the slurry, which might also prevent crusting. The relative effect of wind speed was approximately equal to the relative change in wind speed and, therefore, decreased with increasing wind speed: it was +89% to +100%, +45% to +50% and +30% to +33% at a rise in wind speed of +100% (e.g. from 0.5 m s^{-1} to 1.0 m s^{-1}), +50% (e.g. from 1.0 m s^{-1} to 1.5 m s^{-1}) and +33% (e.g. from 1.5 m s^{-1} to 2.0 m s^{-1}), respectively. The effect size of wind speed was slightly higher at TAA ≤1 d and 1–14 d compared to TAA ≥14 d.

A lower effect in relative terms does not necessarily imply a smaller emission change in absolute figures. For example, the rise in emission for TAA ≤1 d per increase of air temperature by 1 °C is larger in absolute figures since the emission level is higher for TAA ≤1 d than for TAA ≥14 d, *ceteris paribus*. The same applies for wind speed. Overall, this means that the emission increase in absolute figures is more pronounced with an uncrusted surface for a rise in wind speed but less strong for a rise in air temperature. This corresponds to the results of Baldé et al. (2018), who found the weakest relationship between air temperature and emission compared to that between wind speed and emission for slurry with a crusted surface over short periods in a summer season. They explained this by the effect of the crust, which acts as a barrier to gas release. Their findings are mostly in line with the outcomes of the present study.

Additionally, we further evaluated the high emission level in spring using the regression model with 0.063 g NH_3 m^{-2} h^{-1} resulting for spring and 0.059 g NH_3 m^{-2} h^{-1} for summer. The calculated difference is smaller than that of the measured values shown in Table 1. This suggests that a part of the variation in the emission is not captured by the regression model, which is indicated by the model's R^2 value equal to 0.60. Hence, other factors not included in the regression analysis could play a role. This is shown in more detail in Supplementary information 6 and 7.

4. Conclusions

The average emission over the two-year measurement period was 0.065 ± 0.110 g NH_3 m^{-2} h^{-1} with a maximum of 1.67 g NH_3 m^{-2} h^{-1}, which is comparable to values given in the literature. The highest emissions occurred in spring due to frequent slurry agitation, which destroyed the natural crust. Annual emissions per unit of TAN were 3.3% of the TAN flow into the store. This is substantially lower than emission factors reported in the literature or used for emission inventories but can be explained by the low residence time of slurry in the store, the TAN flow into the store, the store surface area and emissions on an area basis. These parameters may vary substantially between farm production systems and, therefore, should be considered for emission factors scaled to the TAN flow into the store.

An increasing period of time after agitation leads to decreasing emissions in dry weather conditions. When combined with a filling level of >1 m, crusting was enhanced due to the higher availability of fibrous material for crust formation, thus inducing a decrease in emissions. Based on the regression analysis, we found a reduction in emissions of 64%–86% due to precipitation, with a greater decrease at a higher intensity. However, the precipitation effect on yearly

emissions is assumed to be limited due to its rather episodic character. Increasing wind speed and temperature enhanced emissions, with the former having a stronger effect. Although the proportion of time without a well-developed natural crust was only 40% of the experimental period, 61% of the total emissions were produced during this time with an average emission of 0.103 g NH_3 m^{-2} h^{-1}. The mean emission from the crusted surface was 0.044 g NH_3 m^{-2} h^{-1}. Thus, to mitigate NH_3 emissions, a natural crust should be preserved by reducing disturbance of the slurry surface.

This study illustrates the complex interactions of influencing factors (storage operations and meteorological conditions) which occur at farm-scale and which require adequate consideration. For future investigations such as the building of models, emission data resolved to measurement intervals together with parameters which reflect the influencing factors are published in Supplementary information 8.

Declaration of competing interest

The authors declare that they have no known competing financial interests or personal relationships that could have appeared to influence the work reported in this paper.

Acknowledgements

Funding by the Office of Waste, Water, Energy and Air, Canton of Zurich (AWEL), Zurich, Switzerland (Contract 1623/21.12.2015) is gratefully acknowledged. We thank the farmer for providing the experimental site and assistance during the measurement campaigns. We are grateful to Albrecht Neftel, NRE, Wohlen, Switzerland, for valuable discussions and revision of the manuscript.

Appendix A. Supplementary data

Supplementary data to this article can be found online at https://doi.org/10.1016/j.biosystemseng.2021.01.001.

REFERENCES

Agafonkin, V., & Thieurmel, B. (2018). *Compute sun position, sunlight phases, moon position and lunar phase*. R package version 0.4. https://CRAN.R-project.org/package=suncalc. (Accessed 24 August 2018).

Baldé, H., VanderZaag, A. C., Burtt, S. D., Wagner-Riddle, C., Evans, L., Gordon, R., et al. (2018). Ammonia emissions from liquid manure storages are affected by anaerobic digestion and solid-liquid separation. *Agricultural and Forest Meteorology, 258*, 80–88.

EEA. (2019). *EMEP/EEA air pollutant emission inventory guidebook 2019. Technical guidance to prepare national emission inventories*. Luxembourg: European Environment Agency.

Efron, B. (1987). Better bootstrap confidence-intervals. *Journal of the American Statistical Association, 82*, 171–185.

Grant, R. H., & Boehm, M. T. (2015). Manure ammonia and hydrogen sulfide emissions from a Western dairy storage basin. *Journal of Environmental Quality, 44*, 127–136.

Grant, R. H., Boehm, M. T., Lawrence, A. F., & Heber, A. J. (2013). Ammonia emissions from anaerobic treatment lagoons at sow and finishing farms in Oklahoma. *Agricultural and Forest Meteorology, 180*, 203–210.

Harper, L. A., Denmead, O. T., & Flesch, T. K. (2011). Micrometeorological techniques for measurement of enteric greenhouse gas emissions. *Animal Feed Science and Technology, 166–67*, 227–239.

Kariyapperuma, K. A., Johannesson, G., Maldaner, L., VanderZaag, A., Gordon, R., & Wagner-Riddle, C. (2018). Year-round methane emissions from liquid dairy manure in a cold climate reveal hysteretic pattern. *Agricultural and Forest Meteorology, 258*, 56–65.

Kupper, T., Bonjour, C., & Menzi, H. (2015). Evolution of farm and manure management and their influence on ammonia emissions from agriculture in Switzerland between 1990 and 2010. *Atmospheric Environment, 103*, 215–221.

Kupper, T., Häni, C., Neftel, A., Kincaid, C., Bühler, M., Amon, B., et al. (2020). Ammonia and greenhouse gas emissions from slurry storage - a review. *Agriculture, Ecosystems & Environment, 300*, 1–18.

Misselbrook, T. H., Brookman, S. K. E., Smith, K. A., Cumby, T., Williams, A. G., & McCrory, D. F. (2005). Crusting of stored dairy slurry to abate ammonia emissions: Pilot-scale studies. *Journal of Environmental Quality, 34*, 411–419.

Ni, J. Q. (1999). Mechanistic models of ammonia release from liquid manure: A review. *Journal of Agricultural Engineering Research, 72*, 1–17.

Nielsen, D. A., Nielsen, L. P., Schramm, A., & Revsbech, N. P. (2010). Oxygen distribution and potential ammonia oxidation in floating, liquid manure crusts. *Journal of Environmental Quality, 39*, 1813–1820.

Petersen, S. O., Dorno, N., Lindholst, S., Feilberg, A., & Eriksen, J. (2013). Emissions of CH_4, N_2O, NH_3 and odorants from pig slurry during winter and summer storage. *Nutrient Cycling in Agroecosystems, 95*, 103–113.

Richner, W., Flisch, R., Mayer, J., Schlegel, P., Zähner, M., & Menzi, H. (2017). 4/Eigenschaften und Anwendung von Düngern. In W. Richner, & S. Sinaj (Eds.), *Grundlagen für die Düngung landwirtschaftlicher Kulturen in der Schweiz/GRUD 2017. Agrarforschung Schweiz 8 (6)* (pp. 4/1–4/23). Spezialpublikation.

Sintermann, J., Dietrich, K., Häni, C., Bell, M. J., Jocher, M., & Neftel, A. (2016). A miniDOAS instrument optimised for ammonia field measurements. *Atmospheric Measurement Techniques, 9*, 2721–2734.

Smith, K., Cumby, T., Lapworth, J., Misselbrook, T., & Williams, A. (2007). Natural crusting of slurry storage as an abatement measure for ammonia emissions on dairy farms. *Biosystems Engineering, 97*, 464–471.

Sommer, S. G., Christensen, M. L., Schmidt, T., & Jensen, L. S. (2013). *Animal manure recycling: Treatment and management*. West Sussex, UK: John Wiley Sons Ltd.

Sommer, S. G., Webb, J., & Hutchings, N. D. (2019). New emission factors for calculation of ammonia volatilization from European livestock manure management systems. *Frontiers in Sustainable Food Systems, 3*, 101.

Sommer, S. G., Zhang, G. Q., Bannink, A., Chadwick, D., Misselbrook, T., Harrison, R., et al. (2006). Algorithms determining ammonia emission from buildings housing cattle and pigs and from manure stores. *Advances in Agronomy, 89*, 261–335.

Sutton, M. A., Oenema, O., Erisman, J. W., Leip, A., van Grinsven, H., & Winiwarter, W. (2011). Too much of a good thing. *Nature, 472*, 159–161.

Therneau, T. (2018). Deming, theil-sen, passing-bablock and total least squares regression. Available online at: https://CRAN.R-project.org/package=deming (09/11/2020).

Thimonier, A., Kosonen, Z., Braun, S., Rihm, B., Schleppi, P., Schmitt, M., et al. (2019). Total deposition of nitrogen in Swiss forests: Comparison of assessment methods and evaluation of changes over two decades. *Atmospheric Environment, 198*, 335–350.

UNECE. (1999). 1999 Protocol to abate acidification, eutrophication and ground-level Ozone to the convention on long-range transboundary air pollution. http://www.unece.org/env/lrtap/multi_h1.html (09.10.2018).

VanderZaag, A., Amon, B., Bittman, S., & Kuczynski, T. (2015). Ammonia abatement with manure storage and processing techniques. In S. Reis, C. Howard, & M. A. Sutton (Eds.), *Costs of ammonia abatement and the climate co-benefits* (pp. 75–112). Springer Netherlands.

VanderZaag, A. C., Gordon, R. J., Glass, V. M., & Jamieson, R. C. (2008). Floating covers to reduce gas emissions from liquid manure storages: A review. *Applied Engineering in Agriculture, 24*, 657–671.

Wood, J. D., Gordon, R. J., Wagner-Riddle, C., Dunfield, K. E., & Madani, A. (2012). Relationships between dairy slurry total solids, gas emissions, and surface crusts. *Journal of Environmental Quality, 41*, 694–704.